We thank the referee for his/her time to provide us with extensive and valuable input. Please find below our responses to the raised comments, questions and suggestions. In the following, raised **comments / suggestions are in red** and respective **responses in green**, while **alterations to the manuscript text are indicated in blue**.

**General Comment**

This manuscript reports a systematic study on the long term chemically-resolved size distribution data measured by a high-resolution AMS from an urban and a suburban location in Hong Kong. Measured size distributions of individual species were fitted using a bimodal lognormal model and the derived mode sizes and submode concentrations were analyzed for seasonal and diurnal variations. Based on these results, the authors discussed the influences of different sources on aerosol sizes, differences between urban and suburban aerosols, and variations in aerosol mixing states. The work reported in this ms is technically sound and interesting and the synthesis of long-term AMS size distribution data is a novel undertaking. However, the assumption that all aerosol size distributions are bimodal appears to be overly simplified and somewhat arbitrary. Urban particles, in particular, are contributed by various primary and secondary sources and particle from different sources tend to have different size distributions. Although I could see the benefit of simplifying the complexity by using a bimodal assumption, it would be helpful that the authors elaborate a bit more on the justification for this treatment and provide more details on how well the biomodal log-normal model perform in fitting the observation data. Maybe a more systematic evaluation of the quality of fit for the size distribution data is more appropriate than one example (Fig. D1). Also, I would like mention that more sophisticated methods, such as the 3-dimentional factor analysis reported in Ulbrich et al. (2012), maybe useful to explore the number of modes. I also notice that the naming of the size modes in this work is a bit confusing. Aitken mode refers to particles smaller than 100 nm in diameter. However, according to Fig. 1 and 2, the mode diameters for the so-called "Aitken mode" determined through bimodal log-normal fitting are all above 100 nm, some even reaching 200 nm. Additionally, the discussions on diurnal variations of aerosol size mode focus very much on the impacts of emissions sources and physical and chemical processes. However, changes of air masses due to wind shifts or upwind impacts could also be important and should be evaluated.

We will present a brief review of AMS-related size distribution work as well as more details for the considerations and procedures involved in the peak fitting in the revised manuscript and Supporting Material. While we agree that especially in more complex urban environments, multimodality in size distributions is likely we can only clearly distinguish two modes in the mass size distributions from our field measurements. The impacts from coarser particles (>$PM_1$) are usually visible as enhanced tails at the upper boundary of the mass size distributions, however, the influence of decreasing lens transmission and possible impacts of longer evaporation times of larger particles (Canagaratna et al., 2004) render further examination unfeasible. Otherwise, there were no clear indications of possible further submodes (e.g. shoulders, peaks, etc.) and fitting of additional modes did not appear warranted, leading to our approach of a bimodal deconvolution.

The naming conventions have been chosen as to capture the overall character of the modes. Bearing in mind that presented particle diameters are in terms of vacuum-aerodynamic diameter, which is related to the more commonly used mobility diameter by approximately a factor of particle density, the resolved mode diameters correspond to mobility diameters around 100-150nm, thus close to the Aitken mode.

We recognize that our Aitken particle mode is in the borderline region between Aitken and accumulation mode and we will clarify the definition more clearly in the introductory and methodology part in the revised manuscript.

For the day-to-day size distributions, we examined wind frequency data and data from backtrajectory analysis (see Figures D12-13 in the Supporting Material). The diurnal analysis is split by seasons and thus encompasses 1-2 months of measurement data. Surface wind patterns at both measurement sites were rather complex and subject to irregular processes (e.g. street canyon effects, land-sea-breeze, monsoon circulation). It is unlikely that air mass changes or wind shifts occurred at regular diurnal time scales at both measurement sites and are therefore not discussed in the context of the diurnal size distributions.

The smaller mode typically exhibited mode diameters in the range of 100-200 nm ($d_{va}$) and is thus in the transition region between Aitken and lower accumulation mode. For a clearer distinction from the larger mode which unambiguously belonged to the accumulation size range, we opt to refer to the small mode as *Aitken mode* in this work.

Associated further changes:

- Addition of Chapter 3.3 to the manuscript, discussing previous studies.
- Revision and addition to Section B of the Supporting Material.

The relevant changes are appended at the bottom of this document

**Specific Comments**

**Comment** The numbering of the sections does not seem logic. For example, according to content, 3.2.1 is parallel to 3.2.

**Response** The numbering of sections in chapter 3 is erroneous. Part 3.2. should in fact be 3.1.1., while 3.2. should be 3.1.2. This also affects section numbers thereafter, and we provide a corrected chapter numbering in the revised manuscript.

**Comment** Line 11 - 12: this sentence is difficult to understand, consider to revise.

**Response** We have revised the concerned sentence.

**Alteration** The size distributions displayed bimodal characteristics and were deconvoluted into submodes which were analyzed for diurnal trends and longer term day-to-day variations.

**Comment** Line 63, the AMS lens transmission is close to zero for particles smaller than 30-35 nm, so it is not precise to say the Aitken mode particles (10-100 nm) are covered by AMS.

**Response** We agree that the AMS inlet lens is not capable of capturing particles in the smallest Aitken mode range which is relevant in terms of particle number concentration. Particle volume and thus particle mass is however dominated by large particles in each mode, and thus the AMS would still be able to capture most of the Aitken mode (from a particle mass perspective), which is mentioned in Line 63 ("particle mass").

**Comment** Line 65 states that the AMS particle size data from ambient measurements are rarely investigated in depth. This is not true. A number of studies, including a few from more than 10 years ago, analyzed the size-resolved composition data from AMS quite extensively and utilized the information to elucidate aerosol sources, new particle formation and growth mechanisms, and other atmospheric processes. Several references (not the complete list) are provided at the end of this comment in the reference section. In addition, Ulbrich et al. (2014) reported a comprehensive study on the size-resolved mass spectral data from an ambient study using 3-D factorization models. Considering that this manuscript focuses on AMS size distribution data, I'd like to recommend that the authors provide a background review on previous works in the introduction. Additionally,I notice that citations are sometime missing when findings from the authors' own research group are mentioned. This could cause confusion when the results from this work alone are sufficient to support the claim. A thorough check for in-text citations is recommended.

**Response** We seek to clarify the sentence concerned (Line 65). We aim to stress that AMS particle size distribution on finer time scales are in fact rarely investigated. The majority of studies examined overall average size distributions i.e. covering the whole sampling campaign, specific episodic event or limited time periods of interest.

We will rephrase this sentence and incorporate a short section reviewing these studies as recommended by the reviewer.

**Alteration** Thus far most studies employing ambient size distribution data from aerosol mass spectrometer measurements investigated longer time period averages, i.e. campaign averages (Salcedo et al., 2006;Sun et al., 2009;Aiken et al., 2009;Huang et al., 2010;Takegawa et al., 2009;Saarikoski et al., 2012;Li et al., 2015) or specific time periods of interest (Elser et al., 2016;Lee et al., 2013). Mohr et al. separated organic particle mass size distributions by periods of dominant influence of different PMF-resolved organic aerosol factors to study the properties of mass size distributions in relation to organic aerosol composition (Mohr et al., 2012). The 3D-factorization technique is an extension of traditional AMS PMF analysis on organic aerosol allowing estimates on the size distributions of organic aerosol factors, however under the assumption that factor size distributions remain invariant over the measurement period (Ulbrich et al., 2012).

The temporal evolution of species-specific size distributions, are mostly discussed qualitatively (Drewnick et al., 2005) and only few studies have evaluated temporal trends in mass size distributions in greater detail. Particle nucleation and subsequent growth events were investigated in Pittsburgh using size data from an AMS and two SMPS as well as various gaseous pollutant instruments and meteorological information. The AMS mass size distributions were evaluated quantitatively using the time series of binned particle

concentrations generated from the grouping of raw data into wider size bins to represent different stages in the particle growth process. (Zhang et al., 2004). The same method was employed to evaluate contributions of ultrafine mode and accumulation mode particles to total organic particle mass (Zhang et al., 2005) by summation of size bins in the range of 30-100 nm and 100-1000nm. The authors also explored diurnal changes in size distributions of particle species by averaging over 3h periods in the morning (6–9 am) and afternoon (1–4 pm). Sun et al. present a qualitative discussion of diurnal variations in the mass size distributions of the m/z 44, m/z 57 and derived $C_4H_9^+$ ion signals from measurements at an urban site in New York (Sun et al., 2011). Similarly, Setyan et al. examined diurnal changes in the mass size distributions of organics and sulfate qualitatively and used binned concentrations (40–120, 120–200, and 200–800) nm in their quantitative analysis to study the evolution of particle chemistry in new particle formation and growth events (Setyan et al., 2012).

**Comment** Line 91, what's the RH at the exit of the dryer?
**Response** The relative humidity at the diffusion drier outlet was consistently in a range of 20-30% and tested periodically in both campaigns.

**Comment** Line 130 - 132, the sentence "Utilizing ..." is vague, consider to revise
**Response** We have revised the sentence.
**Alteration** AMS mass-based size distributions can be utilized more systematically and complementary to standard AMS data analysis techniques by deconvoluting multimodal distributions into their constituting submodes and evaluating their variation and contribution to overall species concentration variations on a diurnal time scale.

**Comment** Line 160, "sweep-out" by what, rain?
**Response** "Sweep out" refers to removal by circulation (e.g. surface wind, traffic induced turbulence), which is particularly important for urban street canyons where periodic changes in circulation (heating, traffic patterns) exist. Washout by rain is another possibility, but is more dependent on specific meteorological conditions, i.e. occurs on irregular basis.

**Comment** Line 161, what's residual traffic?
**Response** We employ the term "residual traffic" in similarity to "background" concentration levels, as traffic in the central inner-city districts remains continuous albeit at much lower vehicle number compared to the daytime, whereas in more remote areas or smaller cities traffic at night is typically intermittent. We will change the wording to avoid confusion.
[…] as well as contributions from nighttime activity such as traffic, which remains continuous in the inner-city districts at night albeit at much lower vehicle numbers compared to the daytime.

**Comment** Line 167 – 169, clarify what the decreases correspond to.
**Response** We have modified the sentence for clarification.
**Alteration** Significant changes were evident in the particle size metric (MMD) during the same time period, where a consistent decrease by 20-30% from about 170 nm (spring) or 160 nm (summer) to 130-140 nm (spring) or 120 nm (summer) was evident with the concurrent increase in road traffic.

**Comment** Line 170- 173, are there SMPS measurements to support the increase of particle number concentrations?
**Response** The measurements presented in this study were conducted with a limited set of available instruments and did unfortunately not encompass complementary particle size distribution measurements (by either electrostatic classification or MOUDI samplers).

**Comment** Line 172, where does the cutoff size of 50 nm come from?
**Response** We here refer to the limitations in AMS lens transmission (see references in Lines 123-124) at the lower size end. The current wording may be confusing and we will revise the sentence to clarify.

**Alteration** […] from elemental carbon particles and smaller Aitken mode and nucleation mode particles below the range of efficient particle transmission of the AMS inlet lens.

**Comment** Line 174 – 190, how important was COA in Aitken mode around noon time? What about contributions from secondary aerosol formation and other primary sources such as HOA? Summertime SOA and SIA formation tend to be higher and can influence particles in all size modes. I am not sure change of cooking behavior was the only reason for the different diurnal shapes between spring and summer.

**Response** As discussed in the captioned section, changes in organic aerosol (as resolved by PMF) during the meal hours were almost exclusively due to changes in COA. Total HOA concentrations beyond the morning rush hour (6:00 – 9:00) remained stable throughout the day and only fell off in the late night hours. Changes in SOA concentrations during the daylight hours were small in both seasons (Lee et al., 2015) and concentration-wise much smaller than daytime COA concentrations. Significant influences from SOA and HOA are thus not likely. Similarly, changes in cooking behavior were not evident, but as mentioned in the captioned section, we consider advection/transport due to differences in wind patterns in spring and summer more likely to be responsible for the observed trend.

**Comment** Line 189 – 190, this sentence is somewhat confusing

**Response** We have revised this sentence for clarification.

**Alteration** Cooking emissions did not lead to conspicuous changes in the size-related distribution metrics, i.e. there were no obvious trends in particle diameters (MMDs) or distribution widths (GSDs) during the meal time periods.

**Comment** Line 213-215, this sentence is confusing. Please clarify.

**Response** This sentence is in support of the previous statement and underlines that meteorological parameters differed substantially between the two seasons. We note that the mentioning of the data source (temperature measurements were taken directly at the roadside station – solar irradiation data were only available from the farther away HKUST site) is not directly relevant to the discussion and may confuse the reader at this point. As the origin of the data is clearly mentioned in the caption of the related Figure, we will omit the information in-text in the revised manuscript.

**Alteration** Ambient temperatures and solar irradiation differed substantially with 7oC higher average temperatures and three times higher integrated daily solar irradiation in summer compared to spring (Figure D6e,f in the Supporting Material).

**Comment** Line 215-216, what does “nucleation of gas-phase emissions” mean?

**Response** The wording is erroneous and has been corrected.

**Alteration** Lower overall ambient temperatures enhance condensation of gas-phase emissions and particle nucleation and shift the gas-to-particle partitioning equilibrium of semi-volatile constituents […]

**Comment** Line 222-223, “reduce nucleation: : : of more volatile exhaust component on fresher, smaller particles: : :”? Did nucleation ever occur with the volatile component in the atmosphere?

**Response** “Reduce” refers to both particle nucleation and, separately, the condensation of volatile exhaust components. We revise this sentence for clarification.

The section in question discusses traffic-exhaust related components from the measurements at the urban roadside location. The site was impacted strongly by vehicle emissions and thus was affected by both nucleation and gas-to-particle conversion from components originating from vehicle exhaust. Both processes are inversely related to temperature. Vehicle exhaust upon discharge from the tailpipe into the ambient atmosphere is rapidly diluted and cooled leading to both gas-to-particle conversion of (semi-)volatile species, homogenous and heterogeneous nucleation and condensation or adsorption on pre-existing particles (Kittelson et al., 2006a;Kittelson et al., 2006b) in the immediate vicinity of the exhaust pipe. The extent of these processes would depend on various parameters including engine type, engine load, species distribution, as well as ambient conditions, e.g. temperature as discussed here.

**Alteration** […] consistent with the expected stronger impact of reduced particle nucleation and reduced condensation of semi-volatile exhaust components on fresher, smaller particles in the warmer season.

**Comment** Line 244-247, this discussion seems somewhat speculative. Are there data to support the nighttime heterogeneous oxidation of SO2 by O3 in Hongkong during spring time? Has this issue been investigated in previous publication(s)? Did wind direction or air mass origin play a role in the observed size mode change?

**Response** Neither wind direction nor air mass origin had any diurnal features that would explain this regularly recurring (i.e. diurnal) observation.
It must be noted that this effect is likely due to the roadside character of the measurement site, leading to ozone peaking during the nighttime (as noted in the manuscript due to NOx titration during the day), and was thus not evident at the suburban measurement site. We are not aware of any detailed investigations into the diurnal concentration characteristics of inorganic components at roadside measurement sites in Hong Kong. The limited amount of additional measurement data beyond gas-phase standard criteria pollutant data unfortunately prevents a deeper analysis in this work.

**Comment** Line 437, "particles containing different species were similar in size" is confusing.
**Response** We have revised the sentence for clarification.
**Alteration** Close nominal agreement (i.e. diameter ratios close to 1) infer that different species were distributed similarly across the particle size range which thus most likely represents a largely internally mixed particle population, while the spread of data (correlation coefficient) indicates the temporal homogeneity or divergence of resolved mode diameters.

**Comment** Line 449, small particles are not just processed by condensational growth and coagulation. In the presence of high humidity, they can also go through aqueous-phase processing.
**Response** We have revised the statement to include the possibility of aqueous-phase processing.
**Alteration** External mixing is more prevalent for freshly formed smaller particles which have typically undergone less atmospheric processing, such as condensational growth, coagulation or aqueous-phase reactions.

**Comment** Fig. D6, can wind data be provided as well?
**Response** Wind patterns at both measurement sites are strongly influenced by irregular processes (street canyon effects, land-sea-breeze, monsoon winds) which typically change from day-to-day. Including diurnal wind data in Figure D6 may thus not be meaningful.

**Changes in sections of main manuscript and Supporting Material**
**Main manuscript**

### 3.3 Comparison to previous studies

Particle size distribution studies in Hong Kong are generally scarce and have focused on either size segregated filter samples (MOUDI) for general ambient measurements or electrostatic classification in particle formation and particle growth studies (Guo et al., 2012;Cheung et al., 2015) . The latter studies focus on specific and narrow time periods and lack general discussions on ambient particle size distributions.

Two ambient studies were undertaken at the suburban coastal HKUST site using size-segregated samples from a ten-stage MOUDI sampler and offline chromatographic analysis. Inorganic constituents (NH4, NO3, SO4) in fine particles (i.e. $D_p$<1.8 µm) were shown to follow bimodal distributions with mode diameters in the range of 0.14-0.21 µm and 0.46-0.58 µm in samples collected in the winter season, while the main mode was observed in the coarse region (4-6 µm) for all three species (Zhuang et al., 1999). A subsequent year-long observational study also reported bimodal fine particle distributions with mode diameters of 0.1-0.3 µm and 0.7–0.9 µm and 1-2 additional modes in the coarse region (Bian et al., 2014), however, the main mode in the size distributions of sulfate, ammonium, potassium and oxalate was observed in the droplet mode (0.7 – 0.9 µm) in this study. Vehicle exhaust plumes sampled on-road from a Mobile Real-time Air Monitoring Platform (MAP) across Hong Kong's road network exhibited three distinct particle volume size distributions: a unimodal distribution with an accumulation mode at 0.2 µm and two bimodal distributions with a minor mode at 0.2 µm and the dominant mode at 0.5 or 0.7 µm (Yao et al., 2007).

The bimodality in the fine particle range across these studies is consistent with the AMS-based results in this work. Nominally, the accumulation mode diameters from filter based studies and the chase studies are larger than those from AMS measurements where maximum mode diameters occurred at $d_{va}$ ~ 700nm, corresponding to $d_a$ ~ 470 (assuming $d_{va}$ ~ $d_a$ * density; particle density ~ 1.5 g/cm$^3$). Direct comparability is however limited due to fundamental differences in sizing techniques (MOUDI: atmospheric pressure; AMS: near-vacuum), sampling times (MOUDI: 24h samples, scattered time line; AMS: minute raw resolution averaged to hourly or daily, continuous time line), measurement uncertainties (MOUDI: sampling artifacts such as vapor adsorption and desorption; AMS: inlet lens transmission) and aerosol pretreatment (none for MOUDI with potential impacts on particle size in high humidity (>80%) conditions (Fang et al., 1991); AMS: removal of water prior to introduction to instrument).

**Supporting Material**

Lognormal peaks were fitted to each 24h and hour-of-day AMS mass size distribution respectively employing the *Multipeak Fit V2* algorithm in *Igor Pro (Wavemetrics)* using a simple vertical offset as the baseline and initial guesses on peak position, height, and width based on visual inspection of the raw size distribution. The multipeak fitting tool employs the Levenberg-Marquardt algorithm (Gill et al., 1981) as a non-linear least squares fit and iteratively adjusts the initial fit parameter guesses until a convergent solution with minimized residuals is achieved. In sporadic cases, the fitted solution led to excessive deviations from the initial guesses with greatly shifted peak locations and large fluctuations in peak width. In such cases, results from the peak fits of immediately adjacent size distributions (i.e. previous and next distributions in the sequence) were evaluated and used to adjust the fitting process by fixing either the location (*primary*) or the width of the peak (*secondary*) to the average value of the two adjacent fitted distributions.

For the diurnal size distributions, measurement data from time periods with large differences in species concentration levels were pooled together. The averaging of mass (or volume) based size distribution involves different uncertainties for each size bin due to the cubic relationship between particle mass (or volume) and particle diameter and the corresponding improvement in signal-to-noise ratio with increasing particle size. To establish reliable diurnal trends we adopt an approach similar to the analysis of conventional species concentration diurnal trends by evaluating size distributions reconstructed from the average, median, 25$^{th}$ and 75$^{th}$ percentile of each size bin. Similar diurnal trends in the fitting parameters across these different size distributions would confirm that changes were indeed recurrent daily while divergent trends would indicate that irregular processes (e.g. episodic events) were more significant in determining size distribution characteristics. Since episodic pollution events and clean periods (e.g. prolonged precipitation) were not removed from the dataset, the quantitative analysis focuses on trends observed in the median dataset to minimize skewing effects of high and low concentration periods.

Uncertainties can arise from the peak fitting process itself. While the bimodality of the size distributions was obvious in most cases (i.e. a main mode with a shoulder towards smaller particle sizes, e.g. Figure D1), accumulation mode particle mass can occasionally dominate the mass size distribution and diminish the Aitken

mode. To achieve confidence in the appropriateness of the bimodal fitting we evaluated both unimodal and bimodal peak fits whenever the Aitken to accumulation mode peak ratio was <10% and we depict a representative example below (Figure D2a. b). The distribution of the fit residuals (Figure D2c, d) was examined and cumulative probability distributions of the fit residuals compared by the Kolmogorov-Smirnov test (Figure D2e) to assess whether fit residuals were significantly different at 95% confidence level (CL). It is evident that the bimodal fit performs better at resolving the raw size distribution in the smaller size region and overall yields a more normal residual distribution. The Kolmogorov-Smirnov test confirms that the residual distributions are statistically different ($D>D_{critical}$ at 95% CL). We tested all borderline cases using the outlined procedure. In this study, bimodal fits yielded unanimously better results in all cases for both diurnal and day-to-day size distributions and all investigated species, i.e. the Aitken mode always remained clearly distinguishable from the accumulation mode.

While the peak fitting algorithm yields a unique individual solution with a set of parameters for which resulting residuals (*difference of fitted and original distribution*) are minimized, the surrounding solution space provides a potentially infinite number of similar solutions with slightly larger residuals. The standard deviations of the fit parameters can provide an estimate of the variability of the peak parameters between the final fit solution and the surrounding solution space. We evaluated the uncertainty in peak area (i.e. integrated mode particle mass) which represents the combined uncertainty of the peak position, width and height (which altogether directly determine the peak area) for all fitted size distributions in this work.

Figure D3 depicts the standard deviation of resolved peak area (i.e. integrated mode particle mass concentration) nominally and relative to the peak area for the diurnal size distributions of NO3 at the urban Mong Kok site in summer 2013 and Tables C1-C2 summarize the values of percent standard deviations for all species at both measurement sites respectively. The median datasets, which were used for quantitative discussion for the diurnal size distribution analysis, exhibited particle mass uncertainties of 14-48% in the Aitken mode and 1-12% in the accumulation mode at the suburban HKUST site, and 7-44% in the Aitken mode and 1-6% in the accumulation mode at the urban MK site. Figure D4 depicts the $75^{th}$ percentile-bin diurnal variation of NO3 (which displayed the largest uncertainties in Figure D3) with the corresponding peak area variability, and shows that the interpretation of the diurnal variation would remain largely unaffected from the incurred uncertainties.

For the day-to-day 24h size distributions a corresponding analysis was undertaken, with Figure D5 depicting the size distributions of NO3 at the HKUST site for all covered seasons exemplarily, and Table C3 summarizes the values of percent standard deviations for all species at both measurement sites respectively. Peak fit uncertainties typically increase with decreasing integrated peak area and can exceed the values of the peak area in the Aitken mode in a small number of cases (e.g. Figure D5c,e – ratios >1). Quantification of the Aitken mode may not be possible at high levels of confidence in these isolated cases. They were retained in the dataset due to their low frequency of occurrence and to enable a complete discussion over the full concentration range without biasing towards larger concentration (i.e. fitted peak areas) values.

**Table C1.** Percentiles of relative standard deviation (*rows; corresponding to the box-whiskers plot in Figure D3e,f*) in percent from lognormal peak fits (bimodal deconvolution) for the resolved Aitken mode (a) and accumulation mode (b) particle concentration for diurnal size distributions at the HKUST supersite (2011/12), *columns* describe the data set, i.e. reconstructed size distributions from the 25th percentile, median, 75th percentile and mean of the size bins
*Sp=Spring, Su=Summer, Fa=Fall, Wi=Winter*

(a)

| Aitken mode | | 25th PC Distr. | | | | Median Distr. | | | | 75th PC Distr. | | | | Mean Distr. | | | | Range |
|---|---|---|---|---|---|---|---|---|---|---|---|---|---|---|---|---|---|---|
| % SD | | Sp | Su | Fa | Wi | Sp | Su | Fa | Wi | Sp | Su | Fa | Wi | Sp | Su | Fa | Wi | |
| NO3 (UST) | PC-90 | 67 | 76 | 39 | 85 | 76 | 44 | 54 | 55 | 80 | 75 | 56 | 39 | 36 | 77 | 44 | 42 | 36-85 |
| | PC-75 | 52 | 42 | 28 | 57 | 66 | 32 | 39 | 40 | 61 | 59 | 44 | 29 | 22 | 38 | 35 | 34 | 22-66 |
| | **PC-50** | **36** | **33** | **22** | **46** | **44** | **26** | **31** | **22** | **40** | **43** | **34** | **23** | **18** | **28** | **24** | **30** | **18-46** |
| | PC-25 | 29 | 25 | 16 | 28 | 26 | 14 | 24 | 18 | 25 | 29 | 22 | 17 | 14 | 19 | 20 | 25 | 14-29 |
| | PC-10 | 21 | 20 | 15 | 24 | 19 | 12 | 19 | 15 | 17 | 19 | 17 | 10 | 13 | 13 | 15 | 21 | 10-24 |
| SO4 (UST) | PC-90 | 38 | 38 | 42 | 74 | 19 | 36 | 39 | 43 | 22 | 40 | 40 | 42 | 19 | 36 | 37 | 81 | 19-81 |
| | PC-75 | 35 | 33 | 38 | 55 | 18 | 28 | 33 | 32 | 18 | 30 | 35 | 64 | 17 | 30 | 30 | 66 | 17-66 |
| | **PC-50** | **28** | **30** | **33** | **32** | **16** | **26** | **27** | **25** | **14** | **24** | **27** | **27** | **14** | **24** | **26** | **48** | **14-48** |
| | PC-25 | 21 | 25 | 26 | 24 | 13 | 21 | 22 | 21 | 11 | 18 | 24 | 22 | 12 | 21 | 23 | 40 | 11-40 |
| | PC-10 | 17 | 23 | 24 | 19 | 11 | 20 | 20 | 13 | 10 | 14 | 20 | 19 | 10 | 19 | 22 | 35 | 10-35 |
| Org (UST) | PC-90 | 52 | 23 | 41 | 44 | 42 | 28 | 32 | 27 | 47 | 48 | 45 | 53 | 46 | 29 | 24 | 32 | 23-53 |
| | PC-75 | 41 | 18 | 26 | 28 | 30 | 22 | 27 | 22 | 26 | 39 | 35 | 44 | 36 | 23 | 21 | 25 | 18-44 |
| | **PC-50** | **26** | **14** | **17** | **21** | **19** | **18** | **21** | **17** | **20** | **32** | **26** | **35** | **23** | **18** | **19** | **21** | **14-35** |
| | PC-25 | 16 | 11 | 13 | 18 | 17 | 16 | 19 | 15 | 18 | 28 | 20 | 29 | 18 | 14 | 16 | 17 | 11-29 |
| | PC-10 | 9 | 9 | 10 | 11 | 14 | 9 | 15 | 12 | 15 | 20 | 17 | 21 | 17 | 11 | 14 | 16 | 9-21 |

(b)

| Accum. mode | | 25th PC Distr. | | | | Median Distr. | | | | 75th PC Distr. | | | | Mean Distr. | | | | Range |
|---|---|---|---|---|---|---|---|---|---|---|---|---|---|---|---|---|---|---|
| % SD | | Sp | Su | Fa | Wi | Sp | Su | Fa | Wi | Sp | Su | Fa | Wi | Sp | Su | Fa | Wi | |
| NO3 (UST) | PC-90 | 8 | 5 | 8 | 4 | 7 | 5 | 6 | 3 | 4 | 9 | 6 | 3 | 3 | 4 | 5 | 1 | 1-9 |
| | PC-75 | 6 | 4 | 7 | 3 | 3 | 4 | 5 | 2 | 4 | 7 | 5 | 2 | 2 | 3 | 5 | 1 | 1-7 |
| | **PC-50** | **4** | **3** | **5** | **2** | **3** | **3** | **5** | **2** | **3** | **4** | **5** | **2** | **2** | **3** | **4** | **1** | **1-5** |
| | PC-25 | 3 | 3 | 4 | 2 | 2 | 3 | 4 | 1 | 3 | 3 | 4 | 2 | 2 | 2 | 4 | 1 | 1-4 |
| | PC-10 | 2 | 2 | 4 | 1 | 2 | 2 | 4 | 1 | 2 | 2 | 3 | 1 | 2 | 2 | 3 | 1 | 1-4 |
| SO4 (UST) | PC-90 | 2 | 3 | 3 | 5 | 2 | 2 | 2 | 3 | 3 | 2 | 3 | 4 | 2 | 2 | 2 | 2 | 2-5 |
| | PC-75 | 2 | 2 | 2 | 2 | 2 | 2 | 2 | 2 | 2 | 2 | 2 | 3 | 1 | 2 | 2 | 2 | 1-3 |
| | **PC-50** | **2** | **2** | **2** | **1** | **2** | **2** | **2** | **2** | **2** | **2** | **2** | **2** | **1** | **2** | **2** | **1** | **1-2** |
| | PC-25 | 2 | 2 | 2 | 1 | 1 | 2 | 2 | 1 | 1 | 2 | 2 | 2 | 1 | 2 | 2 | 1 | 1-2 |
| | PC-10 | 1 | 2 | 1 | 1 | 1 | 2 | 2 | 1 | 1 | 1 | 2 | 1 | 1 | 2 | 2 | 1 | 1-2 |
| Org (UST) | PC-90 | 29 | 12 | 16 | 9 | 18 | 8 | 9 | 5 | 10 | 6 | 7 | 3 | 18 | 7 | 5 | 5 | 3-29 |
| | PC-75 | 18 | 9 | 11 | 7 | 10 | 5 | 5 | 3 | 6 | 4 | 5 | 2 | 11 | 5 | 4 | 3 | 2-18 |
| | **PC-50** | **12** | **7** | **5** | **5** | **6** | **4** | **4** | **3** | **4** | **3** | **4** | **2** | **7** | **3** | **3** | **3** | **2-12** |
| | PC-25 | 7 | 4 | 3 | 3 | 5 | 3 | 3 | 2 | 3 | 2 | 3 | 2 | 5 | 2 | 2 | 2 | 2-7 |
| | PC-10 | 4 | 4 | 1 | 2 | 4 | 2 | 2 | 1 | 2 | 2 | 2 | 1 | 2 | 1 | 2 | 2 | 1-4 |

**Table C2.** Percentiles of relative standard deviation (*rows; corresponding to the box-whiskers plot in Figure D3e,f*) in percent from lognormal peak fits (bimodal deconvolution) for the resolved Aitken mode (a) and accumulation mode (b) particle concentration for diurnal size distributions at the urban MK site (2013), *columns* describe the data set, i.e. reconstructed size distributions from the 25th percentile, median, 75th percentile and mean of the size bins *Sp=Spring, Su=Summer*

(a)

| Aitken mode % SD | | 25th PC Distr. | | Median Distr. | | 75th PC Distr. | | Mean Distr. | | Range |
|---|---|---|---|---|---|---|---|---|---|---|
| | | Sp | Su | Sp | Su | Sp | Su | Sp | Su | |
| NO3 (MK) | PC-90 | 38 | 46 | 40 | 34 | 40 | 41 | 22 | 26 | 22-46 |
| | PC-75 | 27 | 34 | 26 | 28 | 34 | 35 | 20 | 16 | 16-35 |
| | **PC-50** | **15** | **24** | **23** | **21** | **25** | **28** | **18** | **14** | **14-28** |
| | PC-25 | 9 | 20 | 19 | 17 | 18 | 22 | 15 | 12 | 9-22 |
| | PC-10 | 6 | 19 | 16 | 14 | 15 | 20 | 13 | 11 | 6-20 |
| SO4 (MK) | PC-90 | 63 | 46 | 35 | 38 | 24 | 31 | 23 | 21 | 21-63 |
| | PC-75 | 50 | 36 | 30 | 36 | 21 | 28 | 21 | 20 | 20-50 |
| | **PC-50** | **44** | **33** | **28** | **24** | **20** | **23** | **19** | **18** | **18-44** |
| | PC-25 | 37 | 27 | 24 | 21 | 17 | 20 | 15 | 17 | 15-37 |
| | PC-10 | 33 | 25 | 21 | 19 | 15 | 18 | 15 | 16 | 15-33 |
| Org (MK) | PC-90 | 22 | 12 | 22 | 19 | 30 | 21 | 15 | 14 | 12-30 |
| | PC-75 | 16 | 10 | 12 | 12 | 18 | 11 | 12 | 8 | 8-18 |
| | **PC-50** | **10** | **8** | **10** | **9** | **10** | **9** | **8** | **7** | **7-10** |
| | PC-25 | 8 | 7 | 8 | 7 | 7 | 8 | 6 | 6 | 6-8 |
| | PC-10 | 7 | 6 | 7 | 6 | 6 | 6 | 5 | 5 | 5-7 |

(b)

| Accum. mode % SD | | 25th PC Distr. | | Median Distr. | | 75th PC Distr. | | Mean Distr. | | Range |
|---|---|---|---|---|---|---|---|---|---|---|
| | | Sp | Su | Sp | Su | Sp | Su | Sp | Su | |
| NO3 (MK) | PC-90 | 9 | 9 | 6 | 7 | 3 | 5 | 2 | 5 | 2-9 |
| | PC-75 | 6 | 8 | 4 | 5 | 3 | 4 | 2 | 4 | 2-8 |
| | **PC-50** | **4** | **6** | **3** | **4** | **2** | **3** | **2** | **3** | **2-6** |
| | PC-25 | 2 | 5 | 2 | 4 | 2 | 3 | 1 | 3 | 1-5 |
| | PC-10 | 2 | 4 | 1 | 3 | 1 | 3 | 1 | 2 | 1-4 |
| SO4 (MK) | PC-90 | 4 | 3 | 2 | 3 | 2 | 5 | 2 | 3 | 2-5 |
| | PC-75 | 3 | 2 | 2 | 3 | 2 | 4 | 2 | 2 | 2-4 |
| | **PC-50** | **3** | **2** | **2** | **2** | **1** | **4** | **2** | **2** | **1-4** |
| | PC-25 | 2 | 2 | 2 | 2 | 1 | 3 | 1 | 2 | 1-3 |
| | PC-10 | 2 | 2 | 1 | 2 | 1 | 3 | 1 | 2 | 1-3 |
| Org (MK) | PC-90 | 9 | 8 | 8 | 7 | 9 | 5 | 6 | 6 | 5-9 |
| | PC-75 | 6 | 7 | 5 | 5 | 5 | 4 | 5 | 4 | 4-7 |
| | **PC-50** | **5** | **5** | **4** | **4** | **3** | **4** | **3** | **4** | **3-5** |
| | PC-25 | 4 | 4 | 3 | 3 | 3 | 3 | 3 | 3 | 3-4 |
| | PC-10 | 2 | 3 | 3 | 3 | 5 | 2 | 2 | 2 | 2-3 |

**Table C3.** Percentiles of percent standard deviation (*rows; corresponding to the box-whiskers plot in Figure D5e,f*) from lognormal peak fits (bimodal deconvolution) for the resolved Aitken mode and accumulation mode for 24h day-to-day size distributions at the suburban HKUST site (a) and the urban MK site (b) for all investigated species, *columns* describe the uncertainties in terms of quartiles of resolved peak area, where Q1 refers to the lowest 25% and Q4 the highest 25% of resolved peak area (see also Figure D4)

(a)

| HKUST '11/12 % SD | | NO3 | | | | | SO4 | | | | | Org | | | | |
|---|---|---|---|---|---|---|---|---|---|---|---|---|---|---|---|---|
| | | Q1 | Q2 | Q3 | Q4 | Range | Q1 | Q2 | Q3 | Q4 | Range | Q1 | Q2 | Q3 | Q4 | Range |
| **Aitken mode** | PC-90 | 95 | 64 | 50 | 27 | 27-95 | 97 | 78 | 49 | 30 | 30-97 | 62 | 37 | 28 | 26 | 26-62 |
| | PC-75 | 58 | 47 | 37 | 24 | 24-58 | 91 | 57 | 36 | 20 | 20-91 | 41 | 24 | 21 | 22 | 21-41 |
| | **PC-50** | **47** | **35** | **25** | **17** | **17-47** | **60** | **39** | **29** | **16** | **16-60** | **30** | **17** | **14** | **17** | **14-30** |
| | PC-25 | 30 | 25 | 20 | 13 | 13-30 | 32 | 26 | 21 | 13 | 13-32 | 25 | 14 | 10 | 12 | 10-25 |
| | PC-10 | 20 | 16 | 15 | 8 | 8-20 | 24 | 18 | 13 | 11 | 11-24 | 16 | 11 | 6 | 7 | 6-16 |
| **Accum. mode** | PC-90 | 31 | 9 | 7 | 4 | 4-31 | 4 | 3 | 3 | 3 | 3-4 | 18 | 11 | 9 | 7 | 7-18 |
| | PC-75 | 13 | 6 | 5 | 3 | 3-13 | 3 | 3 | 3 | 2 | 2-3 | 9 | 7 | 6 | 5 | 5-9 |
| | **PC-50** | **8** | **4** | **3** | **2** | **2-8** | **2** | **2** | **2** | **2** | **~2** | **6** | **4** | **5** | **3** | **3-6** |
| | PC-25 | 3 | 3 | 2 | 2 | 2-3 | 2 | 2 | 2 | 2 | ~2 | 4 | 3 | 3 | 2 | 2-4 |
| | PC-10 | 1 | 2 | 2 | 1 | 1-2 | 2 | 2 | 2 | 1 | 1-2 | 3 | 2 | 2 | 2 | 2-3 |

(b)

| MK '13 % SD | | NO3 | | | | | SO4 | | | | | Org | | | | |
|---|---|---|---|---|---|---|---|---|---|---|---|---|---|---|---|---|
| | | Q1 | Q2 | Q3 | Q4 | Range | Q1 | Q2 | Q3 | Q4 | Range | Q1 | Q2 | Q3 | Q4 | Range |
| **Aitken mode** | PC-90 | 62 | 52 | 47 | 30 | 30-62 | 94 | 50 | 29 | 24 | 24-94 | 23 | 17 | 13 | 16 | 13-23 |
| | PC-75 | 41 | 42 | 30 | 25 | 25-42 | 47 | 35 | 22 | 16 | 16-47 | 16 | 14 | 11 | 12 | 11-16 |
| | **PC-50** | **28** | **34** | **21** | **18** | **18-34** | **33** | **24** | **17** | **12** | **12-33** | **11** | **10** | **6** | **8** | **6-11** |
| | PC-25 | 21 | 22 | 19 | 12 | 12-22 | 26 | 17 | 13 | 9 | 9-26 | 8 | 7 | 5 | 6 | 5-8 |
| | PC-10 | 6 | 10 | 13 | 8 | 6-13 | 19 | 14 | 10 | 5 | 5-19 | 6 | 5 | 3 | 3 | 3-6 |
| **Accum. mode** | PC-90 | 22 | 21 | 6 | 6 | 6-22 | 7 | 6 | 6 | 4 | 4-7 | 13 | 8 | 9 | 8 | 8-13 |
| | PC-75 | 17 | 10 | 5 | 3 | 3-17 | 4 | 4 | 4 | 2 | 2-4 | 8 | 7 | 6 | 4 | 4-8 |
| | **PC-50** | **10** | **6** | **4** | **2** | **2-10** | **3** | **2** | **2** | **1** | **1-3** | **6** | **5** | **4** | **2** | **2-6** |
| | PC-25 | 6 | 3 | 2 | 2 | 2-6 | 2 | 2 | 1 | 1 | 1-2 | 4 | 4 | 3 | 2 | 2-4 |
| | PC-10 | 3 | 1 | 2 | 1 | 1-3 | 1 | 1 | 1 | 1 | ~1 | 2 | 3 | 2 | 1 | 1-3 |

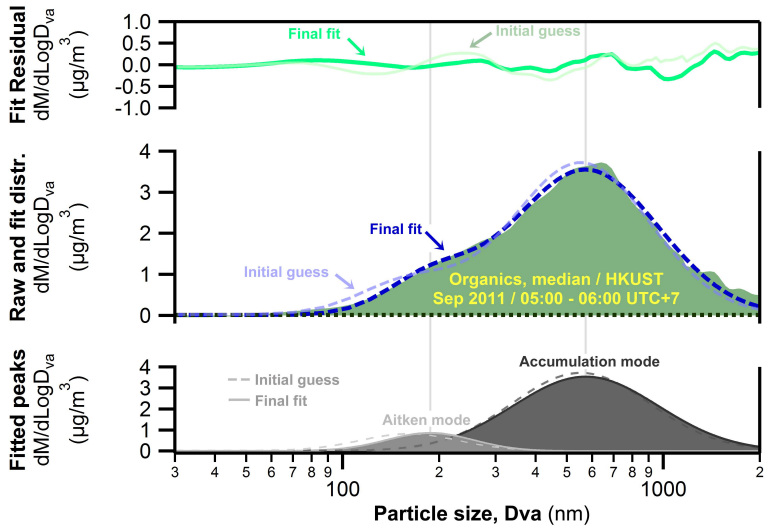


**Figure D1.** Example of a log-normal peak fit *(Multipeak Fit V2, Igor Pro, Wavemetrics, Levenberg-Marquardt algorithm)* of an AMS organics size distribution

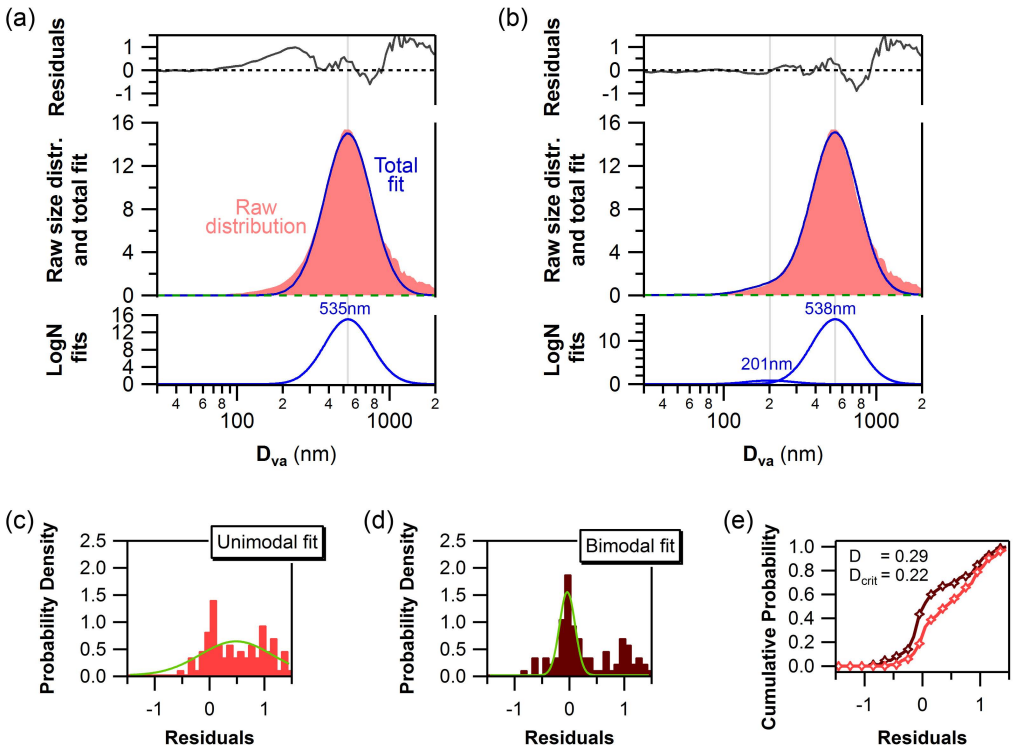


**Figure D2.** 24h average size distribution of sulfate (12/12/2011, suburban HKUST site) with (a) unimodal and (b) bimodal logN peak fitting applied; histograms of residuals from the unimodal (c) and bimodal (d) distributions with Gaussian fit (green); and cumulative probability density functions of uni- and bimodal fit residuals (e) with Kolmogorov-Smirnov D metric values at 95% confidence level

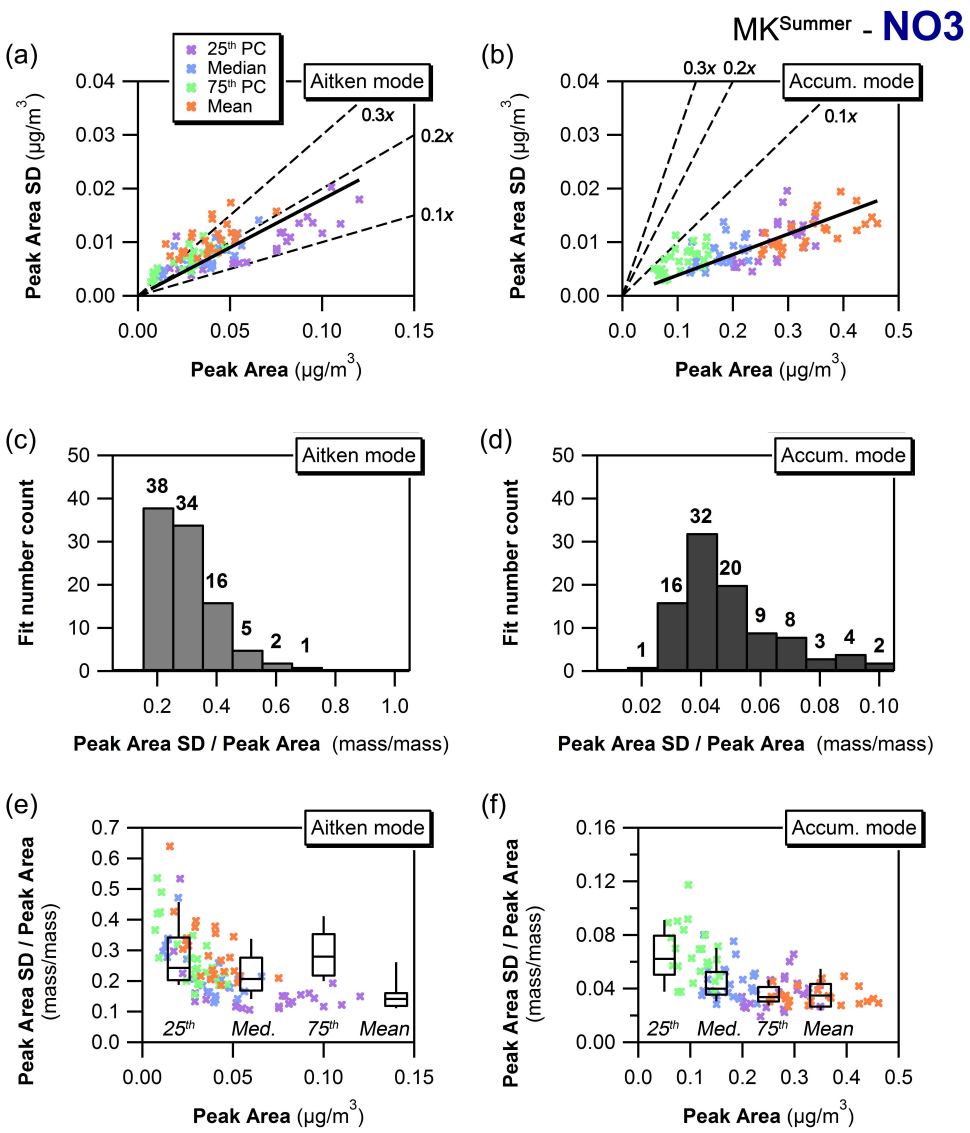


**Figure D3.** Standard deviation of peak area as a function of mode peak area (a,b), histogram of relative standard deviation i.e. the ratio of standard deviation to mode peak area (c,d) where the last bin also contains all values beyond the last bin range, and relative standard deviation as a function of mode peak area (e,f) for the fitted Aitken and accumulation mode with binned box-whiskers plot ($25^{th}$ to $75^{th}$ PC box with horizontal median line and $10^{th}$ to $90^{th}$ PC whiskers where bins refer to quartiles of peak area from lowest Q1 to highest Q4); data for diurnal size distributions of NO3 at the urban Mong Kok site in summer 2013.

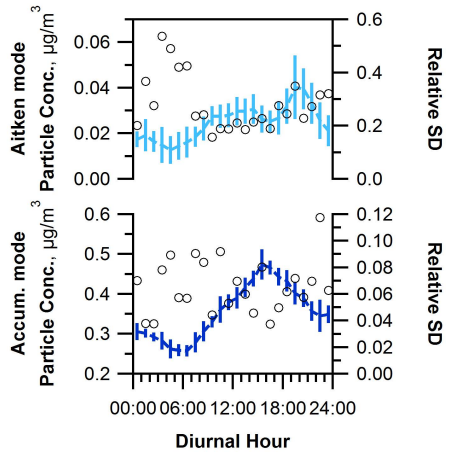


**Figure D4.** Plot of 75$^{th}$ percentile-bin diurnal variation with peak area fit variability and relative standard deviation (corresponding to green data and second to last box in Figure D3e,f)

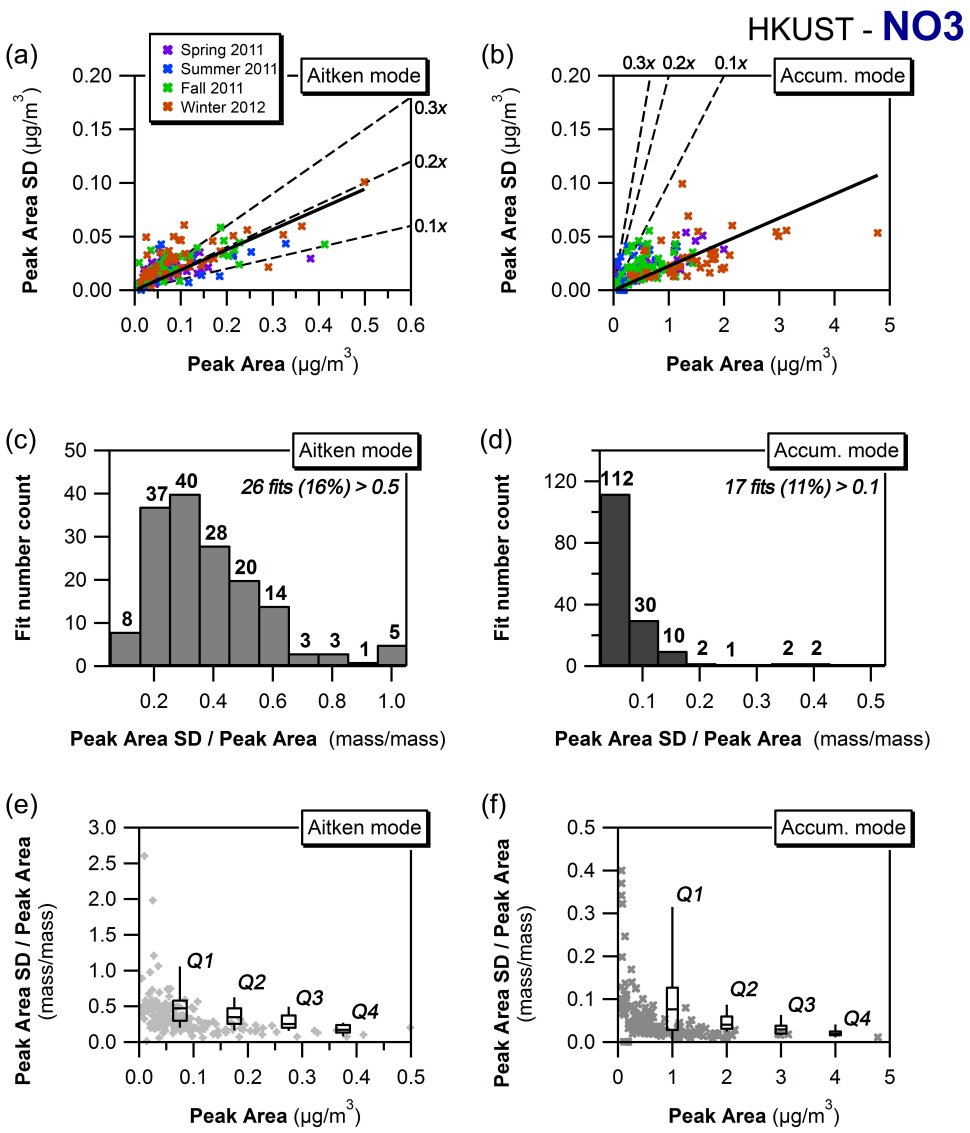


**Figure D5.** Standard deviation of peak area as a function of mode peak area (a,b), histogram of relative standard deviation i.e. the ratio of standard deviation to mode peak area (c,d) where the last bin also contains all values beyond the last bin range, and relative standard deviation as a function of mode peak area (e,f) for the fitted Aitken and accumulation mode with binned box-whiskers plot (25$^{th}$ to 75$^{th}$ PC box with horizontal median line and 10$^{th}$ to 90$^{th}$ PC whiskers where bins refer to quartiles of peak area from lowest Q1 to highest Q4); data for day-to-day size distributions of NO3 at the HKUST site including all seasons.

## References


Aiken, A. C., Salcedo, D., Cubison, M. J., Huffman, J. A., DeCarlo, P. F., Ulbrich, I. M., Docherty, K. S., Sueper, D., Kimmel, J. R., Worsnop, D. R., Trimborn, A., Northway, M., Stone, E. A., Schauer, J. J., Volkamer, R. M., Fortner, E., de Foy, B., Wang, J., Laskin, A., Shutthanandan, V., Zheng, J., Zhang, R., Gaffney, J., Marley, N. A., Paredes-Miranda, G., Arnott, W. P., Molina, L. T., Sosa, G., and Jimenez, J. L.: Mexico City aerosol analysis during MILAGRO using high resolution aerosol mass spectrometry at the urban supersite (T0) - Part 1: Fine particle composition and organic source apportionment, Atmospheric Chemistry and Physics, 9, 6633-6653, 2009.

Bian, Q., Huang, X. H. H., and Yu, J. Z.: One-year observations of size distribution characteristics of major aerosol constituents at a coastal receptor site in Hong Kong – Part 1: Inorganic ions and oxalate, Atmos. Chem. Phys., 14, 9013-9027, 10.5194/acp-14-9013-2014, 2014.

Canagaratna, M. R., Jayne, J. T., Ghertner, D. A., Herndon, S., Shi, Q., Jimenez, J. L., Silva, P. J., Williams, P., Lanni, T., Drewnick, F., Demerjian, K. L., Kolb, C. E., and Worsnop, D. R.: Chase studies of particulate emissions from in-use New York City vehicles, Aerosol Science and Technology, 38, 555-573, 10.1080/02786820490465504, 2004.

Cheung, K., Ling, Z. H., Wang, D. W., Wang, Y., Guo, H., Lee, B., Li, Y. J., and Chan, C. K.: Characterization and source identification of sub-micron particles at the HKUST Supersite in Hong Kong, Science of The Total Environment, 527–528, 287-296, http://dx.doi.org/10.1016/j.scitotenv.2015.04.087, 2015.

Drewnick, F., Hings, S. S., DeCarlo, P., Jayne, J. T., Gonin, M., Fuhrer, K., Weimer, S., Jimenez, J. L., Demerjian, K. L., Borrmann, S., and Worsnop, D. R.: A new time-of-flight aerosol mass spectrometer (TOF-AMS) - Instrument description and first field deployment, Aerosol Science and Technology, 39, 637-658, 10.1080/02786820500182040, 2005.

Elser, M., Huang, R. J., Wolf, R., Slowik, J. G., Wang, Q., Canonaco, F., Li, G., Bozzetti, C., Daellenbach, K. R., Huang, Y., Zhang, R., Li, Z., Cao, J., Baltensperger, U., El-Haddad, I., and Prévôt, A. S. H.: New insights into PM2.5 chemical composition and sources in two major cities in China during extreme haze events using aerosol mass spectrometry, Atmos. Chem. Phys., 16, 3207-3225, 10.5194/acp-16-3207-2016, 2016.

Gill, P. E., Murray, W., and Wright, M. H.: The Levenberg-Marquardt method, in: Practical optimization, Academic Press, London, 1981.

Guo, H., Wang, D. W., Cheung, K., Ling, Z. H., Chan, C. K., and Yao, X. H.: Observation of aerosol size distribution and new particle formation at a mountain site in subtropical Hong Kong, Atmos. Chem. Phys., 12, 9923-9939, 10.5194/acp-12-9923-2012, 2012.

Huang, X. F., He, L. Y., Hu, M., Canagaratna, M. R., Sun, Y., Zhang, Q., Zhu, T., Xue, L., Zeng, L. W., Liu, X. G., Zhang, Y. H., Jayne, J. T., Ng, N. L., and Worsnop, D. R.: Highly time-resolved chemical characterization of atmospheric submicron particles during 2008 Beijing Olympic Games using an Aerodyne High-Resolution Aerosol Mass Spectrometer, Atmospheric Chemistry and Physics, 10, 8933-8945, 10.5194/acp-10-8933-2010, 2010.

Kittelson, D. B., Watts, W. F., and Johnson, J. P.: On-road and laboratory evaluation of combustion aerosols—Part1: Summary of diesel engine results, Journal of Aerosol Science, 37, 913-930, http://dx.doi.org/10.1016/j.jaerosci.2005.08.005, 2006a.

Kittelson, D. B., Watts, W. F., Johnson, J. P., Schauer, J. J., and Lawson, D. R.: On-road and laboratory evaluation of combustion aerosols—Part 2, Journal of Aerosol Science, 37, 931-949, http://dx.doi.org/10.1016/j.jaerosci.2005.08.008, 2006b.

Lee, B. P., Li, Y. J., Yu, J. Z., Louie, P. K. K., and Chan, C. K.: Physical and chemical characterization of ambient aerosol by HR-ToF-AMS at a suburban site in Hong Kong during springtime 2011, Journal of Geophysical Research: Atmospheres, 118, 8625-8639, 10.1002/jgrd.50658, 2013.

Lee, B. P., Li, Y. J., Yu, J. Z., Louie, P. K. K., and Chan, C. K.: Characteristics of submicron particulate matter at the urban roadside in downtown Hong Kong—Overview of 4 months of continuous high-resolution aerosol mass spectrometer measurements, Journal of Geophysical Research: Atmospheres, 120, 7040-7058, 10.1002/2015JD023311, 2015.

Li, Y. J., Lee, B. P., Su, L., Fung, J. C. H., and Chan, C. K.: Seasonal characteristics of fine particulate matter (PM) based on high resolution time-of-flight aerosol mass spectrometric (HR-ToF-AMS) measurements at the HKUST Supersite in Hong Kong, Atmos. Chem. Phys., 15, 37-53, doi:10.5194/acp-15-37-2015, 2015.

Mohr, C., DeCarlo, P. F., Heringa, M. F., Chirico, R., Slowik, J. G., Richter, R., Reche, C., Alastuey, A., Querol, X., Seco, R., Peñuelas, J., Jiménez, J. L., Crippa, M., Zimmermann, R., Baltensperger, U., and Prévôt, A. S. H.:

Identification and quantification of organic aerosol from cooking and other sources in Barcelona using aerosol mass spectrometer data, Atmos. Chem. Phys., 12, 1649-1665, 10.5194/acp-12-1649-2012, 2012.

Saarikoski, S., Carbone, S., Decesari, S., Giulianelli, L., Angelini, F., Canagaratna, M., Ng, N. L., Trimborn, A., Facchini, M. C., Fuzzi, S., Hillamo, R., and Worsnop, D.: Chemical characterization of springtime submicrometer aerosol in Po Valley, Italy, Atmos. Chem. Phys., 12, 8401-8421, 10.5194/acp-12-8401-2012, 2012.

Salcedo, D., Onasch, T. B., Dzepina, K., Canagaratna, M. R., Zhang, Q., Huffman, J. A., DeCarlo, P. F., Jayne, J. T., Mortimer, P., Worsnop, D. R., Kolb, C. E., Johnson, K. S., Zuberi, B., Marr, L. C., Volkamer, R., Molina, L. T., Molina, M. J., Cardenas, B., Bernabe, R. M., Marquez, C., Gaffney, J. S., Marley, N. A., Laskin, A., Shutthanandan, V., Xie, Y., Brune, W., Lesher, R., Shirley, T., and Jimenez, J. L.: Characterization of ambient aerosols in Mexico City during the MCMA-2003 campaign with Aerosol Mass Spectrometry: results from the CENICA Supersite, Atmospheric Chemistry and Physics, 6, 925-946, 2006.

Setyan, A., Zhang, Q., Merkel, M., Knighton, W. B., Sun, Y., Song, C., Shilling, J. E., Onasch, T. B., Herndon, S. C., Worsnop, D. R., Fast, J. D., Zaveri, R. A., Berg, L. K., Wiedensohler, A., Flowers, B. A., Dubey, M. K., and Subramanian, R.: Characterization of submicron particles influenced by mixed biogenic and anthropogenic emissions using high-resolution aerosol mass spectrometry: results from CARES, Atmos. Chem. Phys., 12, 8131-8156, 10.5194/acp-12-8131-2012, 2012.

Sun, Y., Zhang, Q., Macdonald, A. M., Hayden, K., Li, S. M., Liggio, J., Liu, P. S. K., Anlauf, K. G., Leaitch, W. R., Steffen, A., Cubison, M., Worsnop, D. R., van Donkelaar, A., and Martin, R. V.: Size-resolved aerosol chemistry on Whistler Mountain, Canada with a high-resolution aerosol mass spectrometer during INTEX-B, Atmos. Chem. Phys., 9, 3095-3111, 10.5194/acp-9-3095-2009, 2009.

Sun, Y. L., Zhang, Q., Schwab, J. J., Demerjian, K. L., Chen, W. N., Bae, M. S., Hung, H. M., Hogrefe, O., Frank, B., Rattigan, O. V., and Lin, Y. C.: Characterization of the sources and processes of organic and inorganic aerosols in New York city with a high-resolution time-of-flight aerosol mass spectrometer, Atmospheric Chemistry and Physics, 11, 1581-1602, 10.5194/acp-11-1581-2011, 2011.

Takegawa, N., Miyakawa, T., Watanabe, M., Kondo, Y., Miyazaki, Y., Han, S., Zhao, Y., van Pinxteren, D., Bruggemann, E., Gnauk, T., Herrmann, H., Xiao, R., Deng, Z., Hu, M., Zhu, T., and Zhang, Y.: Performance of an Aerodyne Aerosol Mass Spectrometer (AMS) during Intensive Campaigns in China in the Summer of 2006, Aerosol Science and Technology, 43, 189-204, 10.1080/02786820802582251, 2009.

Ulbrich, I. M., Canagaratna, M. R., Cubison, M. J., Zhang, Q., Ng, N. L., Aiken, A. C., and Jimenez, J. L.: Three-dimensional factorization of size-resolved organic aerosol mass spectra from Mexico City, Atmos. Meas. Tech., 5, 195-224, 10.5194/amt-5-195-2012, 2012.

Yao, X., Lau, N. T., Chan, C. K., and Fang, M.: Size distributions and condensation growth of submicron particles in on-road vehicle plumes in Hong Kong, Atmospheric Environment, 41, 3328-3338, 10.1016/j.atmosenv.2006.12.044, 2007.

Zhang, Q., Stanier, C. O., Canagaratna, M. R., Jayne, J. T., Worsnop, D. R., Pandis, S. N., and Jimenez, J. L.: Insights into the chemistry of new particle formation and growth events in Pittsburgh based on aerosol mass spectrometry, Environmental Science & Technology, 38, 4797-4809, 10.1021/es035417u, 2004.

Zhang, Q., Canagaratna, M. R., Jayne, J. T., Worsnop, D. R., and Jimenez, J. L.: Time- and size-resolved chemical composition of submicron particles in Pittsburgh: Implications for aerosol sources and processes, Journal of Geophysical Research-Atmospheres, 110, D07s09 Artn d07s09, 2005.

Zhuang, H., Chan, C. K., Fang, M., and Wexler, A. S.: Size distributions of particulate sulfate, nitrate, and ammonium at a coastal site in Hong Kong, Atmospheric Environment, 33, 843-853, 10.1016/s1352-2310(98)00305-7, 1999.